

# Structure of Butanol and Hexanol at Aqueous, Ammonium Bisulfate, and Sulfuric Acid Solution Surfaces Investigated by Vibrational Sum Frequency Generation Spectroscopy<sup>†</sup>

Lisa L. Van Loon, Rena N. Minor, and Heather C. Allen\*

Department of Chemistry, The Ohio State University, 100 West 18th Avenue, Columbus, Ohio 43210

Received: January 24, 2007; In Final Form: May 6, 2007

The organization of 1-butanol and 1-hexanol at the air–liquid interface of aqueous, aqueous ammonium bisulfate, and sulfuric acid solutions was investigated using vibrational broad bandwidth sum frequency generation spectroscopy. There is spectroscopic evidence supporting the formation of centrosymmetric structures at the surface of pure butanol and pure hexanol. At aqueous, ammonium bisulfate, and at most sulfuric acid solution surfaces, butanol molecules organize in all-trans conformations. This suggests that butanol self-aggregates. The spectrum for the 0.052 M butanol in 59.5 wt % sulfuric acid solution is different from the other butanol solution spectra, that is, the surface butanol molecules are observed to possess a significant number of gauche defects. Relative to surface butanol, surface hexanol chains are more disordered at the surface of their respective solutions. Statistically, an increase in the number of gauche defects is expected for hexanol relative to butanol, a six carbon chain vs a four carbon chain. Yet, self-aggregation of hexanol at its aqueous solution surfaces is not ruled out because the methylene spectral contribution is relatively small. The surface spectra for butanol and hexanol also show evidence for salting out from the ammonium bisulfate solutions.

## Introduction

The uptake of volatile organics by tropospheric aerosols is a possible mechanism for aerosol growth.<sup>1</sup> Recent field measurements show that aerosols and cloud droplets can contain organic compounds from 20% to 70% by mass.<sup>2–4</sup> And recent field campaigns have detected a large number of short-chained oxygenated compounds present in tropospheric aerosols.<sup>5</sup> A decrease in surface tension relative to that of pure water has been observed in wet aerosol and cloud/fog samples<sup>2</sup> suggesting that organic compounds are present at the surfaces of aerosols. This is important since the presence of organic compounds at the surface may change the uptake capabilities and hygroscopicity of aerosols, affecting aerosol growth and ultimately cloud albedo.<sup>6,3,7</sup>

It has long been known that long-chain surfactants are able to form monolayers at the surface of water.<sup>8,9</sup> However, the ordering of shorter, more soluble alcohols such as butanol and hexanol at the surface of aqueous–alcohol mixtures is not yet well understood.<sup>10,11</sup> Inorganic species such as sulfuric acid and ammonium sulfate salts have also long been known to be the predominant fraction of tropospheric aerosols.<sup>12</sup> At the surface of acidic solutions, the orientation of short-chained organics is even more poorly characterized.<sup>10,13</sup> The structure of the short-chain surfactant layer is likely to be important in the ability of the underlying aqueous solvent to absorb gas-phase compounds. Monte Carlo simulations found that the hexanol hydroxyl groups hydrogen bond with water molecules at the 1-hexanol–water interface.<sup>14</sup> Packing of the hexanol molecules allowed for minimal water penetration into the alkyl chain region suggesting that hexanol impedes the evaporation of water from the bulk.

A configurational bias Monte Carlo simulation of 1-butanol on water showed that the butanol monolayer has an excess of surface hydrogen bond acceptor sites in the subsurface layer.<sup>15</sup>

Recent molecular beam experiments showed that the presence of butanol films does not impede the evaporation of water from sulfuric acid solutions.<sup>16</sup> The uptake of HCl and HBr gases is enhanced with the butanol hydroxyl groups providing basic sites available for protonation by the acids.<sup>17</sup> However, the evaporation of H<sub>2</sub>O from 56 to 60 wt % D<sub>2</sub>SO<sub>4</sub> is impeded by the presence of a hexanol film. The hexanol film also raises the entry probability of HCl and HBr into 60 wt % D<sub>2</sub>SO<sub>4</sub>.<sup>10</sup> In another study, the presence of millimolar hexanoic acid concentrations reduced the uptake of N<sub>2</sub>O<sub>5</sub> by artificial seawater by a factor of 3–4.<sup>18</sup> These results suggest that there are differences in the surface structure of butanol and hexanol solutions.

In this study, the organization of butanol and hexanol molecules at the air–liquid interface of aqueous, aqueous ammonium bisulfate, and sulfuric acid solutions was investigated using vibrational sum frequency generation (VSFG) spectroscopy. Butanol and hexanol were chosen due to questions arising from the recent studies mentioned above.<sup>10,16,17</sup> After providing a brief overview of VSFG theory, experimental details including fitting procedures are presented, and then in the Results section, VSFG spectral assignments are provided. (Spectral fits are shown in the Supporting Information.) The Discussion presents the interpretation of the spectra in terms of organization at the surface beginning with neat alcohol comparisons.

Chemical abbreviations used in this paper are BuOH (butanol), HexOH (hexanol), and SA (sulfuric acid). In addition, vibrational sum frequency generation (VSFG), broad bandwidth sum frequency generation (BBSFG), symmetric stretch (ss), and asymmetric stretch (as) are used.

<sup>†</sup> Part of the “Roger E. Miller Memorial Issue”.

\* Corresponding author e-mail: allen@chemistry.ohio-state.edu.

## Experimental Section

**Sum Frequency Generation Spectroscopy.** VSG is a surface selective technique. It is a second-order nonlinear optical technique sensitive to environments lacking inversion symmetry. It has been used to study, among others, solid and liquid surfaces with atmospheric relevance.<sup>19–23</sup> It is sensitive to both the number density and the molecular orientation of the molecules at the interface. Thorough treatments of VSG theory can be found in the literature<sup>24–27</sup> and a brief introduction is given here.

The intensity of the SFG signal,  $I_{\text{SFG}}$ , is proportional to the absolute square of the macroscopic nonlinear susceptibility,  $\chi^{(2)}$ , and to the intensity of the infrared and 800 nm incident beams, eq 1.

$$I_{\text{SFG}} \propto |\chi^{(2)}|^2 I(\omega_{\text{IR}}) I(\omega_{800}) \quad (1)$$

The macroscopic nonlinear susceptibility,  $\chi^{(2)}$ , is described by a nonresonant term,  $\chi_{\text{NR}}^{(2)}$ , and the sum of the resonant terms,  $\chi_{\nu}^{(2)}$ , eq 2.

$$|\chi^{(2)}|^2 = |\chi_{\text{NR}}^{(2)} + \sum_{\nu} \chi_{\nu}^{(2)}|^2 \quad (2)$$

When the frequency of the incident infrared beam is resonant with a vibrational mode,  $\nu$ , then the resonant term dominates the nonlinear susceptibility. The resonant susceptibility term,  $\chi_{\nu}^{(2)}$ , is related to the number density of the surface species and to the molecular hyperpolarizability,  $\beta_{\nu}$ , through the orientationally averaged Euler angle transformation,  $\langle \mu_{\text{IJK:lmn}} \rangle$ , between the laboratory coordinates (IJK) and the molecular coordinates (lmn), eq 3.

$$\chi_{\nu}^{(2)} = N \sum_{lmn} \langle \mu_{\text{IJK:lmn}} \rangle \beta_{\nu}^{lmn} \quad (3)$$

The molecular hyperpolarizability is proportional to the infrared transition moment,  $\mu$ , and the Raman polarizability tensor,  $\alpha$ , showing that SFG active modes must be both Raman- and IR-active, eq 4.

$$\beta_{\nu}^{lmn} = \frac{-\mu_{\nu 0}^n \langle \alpha_{\nu 0}^{lm} \rangle}{2\hbar(\omega_{\nu} - \omega_{\text{IR}} - i\Gamma_{\nu})} \quad (4)$$

From eq 4, the resonant macroscopic nonlinear susceptibility is shown in eq 5.

$$\chi_{\nu}^{(2)} \propto \frac{A_{\nu}}{\omega_{\text{IR}} - \omega_{\nu} + i\Gamma_{\nu}} \quad (5)$$

In the above equation,  $A_{\nu}$  is the strength of the transition moment and  $\omega_{\nu}$  is the frequency of the transition.

From eqs 4 and 5, it becomes clear that only noncentrosymmetric systems, such as the air–liquid interface, will be SFG-active. When the frequency of a vibrational mode,  $\omega_{\nu}$ , is resonant with the infrared frequency,  $\omega_{\text{IR}}$ , the denominator in eq 5 becomes small and  $\beta_{\nu}$ , and therefore  $\chi_{\nu}^{(2)}$ , will be enhanced. A VSG spectrum results from the nonlinear response over the frequency range probed.

The average orientation of the terminal methyl group for butanol,  $\theta_{\text{CH}_3}$ , and the average chain tilt,  $\alpha$ , of the surface butanol molecules when assuming an all-trans conformation were calculated.  $\theta_{\text{CH}_3}$  is calculated from the ratio of the square roots of the intensity of the  $\text{CH}_3$ -ss in the ssp and ppp polarization

spectra.<sup>24,28</sup> The obtained ratio is related to the orientation angle,  $\theta_{\text{CH}_3}$ , as shown in eq 6.

$$\sqrt{\frac{I_{\text{CH}_3\text{-ss,ssp}}}{I_{\text{CH}_3\text{-ss,ppp}}}} = \frac{d_{\text{ss-ssp}}^2 R(\theta)}{d_{\text{ss-ppp}}^2 R(\theta)} \quad (6)$$

where

$$R(\theta) = |\langle \cos \theta \rangle - c \langle \cos^3 \theta \rangle|^2 \quad (7)$$

The parameters  $d$  and  $c$  are defined using the Fresnel coefficients, the hyperpolarizability ratio, the molecular hyperpolarizability, and the related Euler angle transformations<sup>29,30</sup> as derived in Wang et al.<sup>28,31,32</sup>

The variable input parameters used in this study (SF, IR, visible beam angles, depolarization ratio, indices of refraction) and an example calculated plot of  $d_{\text{ss-ssp}}^2 R(\theta)/d_{\text{ss-ppp}}^2 R(\theta)$  vs  $\theta$  are available in Supporting Information. The calculated average orientation angles for neat butanol and the butanol solutions are also found in the Supporting Information. It is assumed that the  $\text{CH}_3$  group has  $C_{3v}$  symmetry, that the surface is isotropic, and that the orientation angle distribution is a  $\delta$  function.<sup>29,30</sup> The average orientation angle of the methyl group in neat butanol is the largest at  $\theta_{\text{CH}_3} = 57^\circ$ . The various butanol solutions have methyl orientation angles ranging from  $39.5^\circ$  to  $48.5^\circ$ . Using the orientation angle of the methyl group, and an angle of  $109^\circ$  between the  $\text{CH}_2$  carbons in the chain, the average tilt angle of the butanol chains is calculated<sup>30,33</sup> to be 4 to  $13^\circ$  from the surface normal using eq 8.

$$\alpha = |35.5 - \theta_{\text{CH}_3}| \quad (8)$$

**BBSFG Instrumentation and Experimental Details.** Details of the broad bandwidth SFG (BBSFG) system can be found in previous publications.<sup>34,35</sup> Briefly, two 1-kHz repetition rate regenerative amplifiers (Spectra Physics Spitfire, femtosecond and picosecond versions) are utilized. The picosecond amplifier produces a narrow bandwidth ( $17 \text{ cm}^{-1}$ ), 2 ps pulse at a wavelength of  $\sim 800 \text{ nm}$ . The femtosecond amplifier is used to pump an optical parametric amplifier (Spectra-Physics OPA 800F) to produce a broad bandwidth,  $\sim 100 \text{ fs}$ , infrared pulse. The spectral window of the IR pulse was  $\sim 450 \text{ cm}^{-1}$  in the C–H stretching region for these experiments. The energy of the 800 nm beam used was  $160\text{--}165 \mu\text{J}$ , and the IR energy in the C–H stretching region was  $5.2\text{--}5.6 \mu\text{J}$  at the sample. The BBSFG experiment was performed in reflection geometry.

The SFG beam is dispersed spectrally in a monochromator (Acton Research, SpectraPro 500i) using a 1200 g/mm diffraction grating blazed at 750 nm. The SFG signal is collected with a CCD detection system (Roper Scientific, LN400EB,  $1340 \times 400$  pixel array, back-illuminated CCD). Spectral resolution was determined to be  $8 \text{ cm}^{-1}$ .<sup>36</sup> Calibration of the CCD camera was completed using the 435.833 nm line from a fluorescent lamp.

Three polarization combinations were used in this study: ssp (s-SFG, s-800 nm, p-infrared), ppp (p-SFG, p-800 nm, p-infrared), and sps (s-SFG, p-800 nm, s-infrared). The polarization of the 800 nm beam is determined by rotation of a zero-order waveplate. By rotation of a  $\text{MgF}_2$  Berek's compensator, the desired IR beam polarization is determined. A glan polarizer in the SFG detection line selects the SFG polarization.

The ssp-polarized spectra were obtained with a 2 min acquisition time. The ppp and sps spectra used 5 min acquisition times. For comparison of the different polarization spectra, the ssp spectra were multiplied by a factor of 5/2. For each solution

and polarization combination, three spectra were obtained. Three background spectra were also obtained by changing the timing of the 800 nm beam. The spectra shown in this paper are the average of the three spectra with the average of three background spectra subtracted. The VSFG spectrum is normalized against a smoothed nonresonant VSFG spectrum from a GaAs crystal to remove any structure present in the IR pulse profile. The dips in a polystyrene–GaAs spectrum are used to calibrate the wavenumber position for each set of experiments.

**Spectral Fitting.** Spectra are fit using the software package IgorPro 4.05. The VSFG spectra are fit with Lorentzian line shapes according to eqs 1 and 5 using IgorPro with user-added fitting functions. The fitting requires user input for the following parameters: two non-resonant terms, the peak amplitudes and phases, peak positions, and peak widths for each component peak. The parameters can be held constant or allowed to vary with the fit. Unless otherwise noted in this work, the parameters were allowed to vary and the peak positions reported are the best fits found with the software. The number of peaks fit corresponds to the number of vibrational modes expected to be SFG-active. The inclusion of a component peak due to the presence of water in the interfacial region was tested in the spectral fitting of the water and  $\text{NH}_4\text{HSO}_4$  solutions and included if it improved the overall fit. Attempts were also made for the butanol in water solutions to include contributions from the asymmetric  $\text{CH}_2$  and  $\text{CH}_3$  modes to the ssp spectra. Further details and examples of the spectral fits are found in the Supporting Information.

**Chemicals.** 1-Butanol (HPLC grade, Fisher Scientific), hexyl alcohol (98%, Acros Organics), sulfuric acid (redistilled, 95.6 wt %, GFS), and ammonium hydrogen sulfate (98%, Aldrich) were used as received. Deionized water was obtained from a Millipore Nanopure system (18.1–18.2  $\text{M}\Omega\cdot\text{cm}$ ).

The 59.5 wt % sulfuric acid solution was prepared by diluting 95.6 wt % sulfuric acid with deionized water. The concentration was determined by titration with a standardized sodium hydroxide solution to  $\pm 0.1$  wt %. The ammonium bisulfate solution was prepared by dissolving the salt in deionized water and filtering two times through a carbon filter (Carbon-Cap 75, Whatman). The concentration ( $0.78 \pm 0.1$  M) was determined spectroscopically using the sulfate vibrational mode at  $985\text{ cm}^{-1}$ . The butanol and hexanol solution concentrations used in this study were chosen to reflect different surface excess conditions.<sup>37</sup> The concentrations and their respective uncertainty used in this study were ( $0.50 \pm 0.02$ ), ( $0.179 \pm 0.003$ ), and ( $0.052 \pm 0.002$ ) M BuOH and ( $0.050 \pm 0.002$ ), ( $0.045 \pm 0.002$ ), ( $0.0099 \pm 0.0003$ ) M, and ( $0.0051 \pm 0.0001$ ) M HexOH.

## Results

While the VSFG spectra of neat alcohols<sup>28,31,32</sup> are found in the literature, much less work has been done to understand the surface structure of aqueous alcohol solutions. Recently the air–liquid interface of aqueous mixtures of methanol, ethanol, and propanol were investigated with VSFG.<sup>11,35,38</sup> The air–liquid interfaces of the longer, but still miscible alcohols (C4, C6) in aqueous, ammonium bisulfate, and sulfuric acid solutions are the focus of this study.

The butanol and hexanol solution concentrations correspond to three different regions of the surface excess curves of 1-butanol in water and 61.5 wt % sulfuric acid solution, and 1-hexanol in 61.5 wt % sulfuric acid solution.<sup>37</sup> The lowest concentrations correspond to a region of low surface excess, far from full surface coverage. The intermediate concentrations correspond to the region where the surface excess is beginning

to level off, slightly less than maximum surface coverage. The greatest concentrations correspond to the region where the surface excess is constant, maximum surface coverage.<sup>37,39,40</sup> The maximum surface coverage for butanol in 61.5 wt % SA is ( $2.25 \pm 0.01$ )  $\times 10^{14}/\text{cm}^2$  and for hexanol is ( $2.80 \pm 0.04$ )  $\times 10^{14}/\text{cm}^2$ .<sup>37</sup> A neutron reflection study<sup>39</sup> found that hexanol forms an open film on a water surface, with the hexanol chains tilted. A molecular dynamics study of a soluble six-atom surfactant chain<sup>40</sup> found that the surface excess plateaus beyond a certain bulk concentration. When increasing from the lowest to the highest concentrations used in these studies, the surface excesses of butanol and hexanol double. All concentrations used in this study were below the solubility limits of the alcohols in water: 115 g/L for 1-butanol and 7.9 g/L for 1-hexanol.<sup>41</sup>

Prior to obtaining the VSFG spectra of the 1-alcohol solution mixtures, the spectra of the neat alcohols were investigated. The neat 1-butanol ssp spectrum, shown in Figure 1a,b, is fit with four component peaks:<sup>28</sup> the  $\text{CH}_2$ -ss at  $2846\text{ cm}^{-1}$ , the  $\text{CH}_3$ -ss at  $2877\text{ cm}^{-1}$ , the  $\text{CH}_2$ -FR at  $2908\text{ cm}^{-1}$ , and the  $\text{CH}_3$ -FR at  $2941\text{ cm}^{-1}$ .

The neat 1-hexanol ssp spectrum, shown in Figure 1f,g, is fit with six component peaks:<sup>28</sup> the  $\text{CH}_2$ -ss at  $2856\text{ cm}^{-1}$ , the  $\text{CH}_3$ -ss at  $2878\text{ cm}^{-1}$ , three  $\text{CH}_2$  Fermi resonances at 2903, 2922, and  $2947\text{ cm}^{-1}$ , and the  $\text{CH}_3$ -FR at  $2939\text{ cm}^{-1}$ .

The ppp and sps polarization spectra of both neat butanol and neat hexanol are shown in Figure 1b,g. The ppp spectra are fit with three component peaks: the  $\text{CH}_3$ -ss, the  $\text{CH}_2$ -as, and the  $\text{CH}_3$ -as. The sps spectra are fit with two component peaks: the  $\text{CH}_2$ -as and the  $\text{CH}_3$ -as. The spectra of neat 1-butanol and neat 1-hexanol in this study are consistent with those found in the literature.<sup>28,31</sup>

The VSFG spectra of butanol in water, aqueous ammonium bisulfate, and SA shown in Figures 1–3 possess four, three, and two component peaks for the ssp, the ppp, and the sps spectra respectively, excluding addition of a broad band attributed to OH stretching of water in the aqueous butanol spectra. For the VSFG spectra of hexanol in water, aqueous ammonium bisulfate, and SA (also shown in Figures 1–3), assignments revealed six, three, and two component peaks for the ssp, the ppp, and the sps spectra respectively. Only the aqueous hexanol solutions included the broad water band, similar to the aqueous butanol solutions. In general, the assignments follow the neat butanol and neat hexanol assignments discussed above. (Peak positions, assignments, and example fits are shown in the Supporting Information.) Of major importance here are the  $\text{CH}_2$ -ss and the  $\text{CH}_3$ -ss denoted by the first two dashed lines in Figures 1–3 (parts b–e and g–j).

## Discussion

The ssp, ppp, and sps VSFG spectra of neat, aqueous, aqueous ammonium bisulfate, and 59.5 wt % SA butanol and hexanol solution surfaces are shown in Figures 1–3. From left to right denoted by dashed lines for Figures 1–3 (parts b–e) and Figures 1–3 (parts g–j) are the  $\text{CH}_2$ -ss, the  $\text{CH}_3$ -ss, the  $\text{CH}_3$ -FR, and the  $\text{CH}_3$ -as, respectively. The  $\text{CH}_3$ -ss peak intensity goes through a maximum in the VSFG spectra for the butanol and hexanol solutions that does not correspond with increasing bulk concentration (or surface excess). Previous studies of short-chain alcohols (C1–C3)<sup>35,11</sup> have shown that the  $\text{CH}_3$ -ss passes through a maximum at a concentration below the solubility limit, as is observed here. This phenomenon is indicative of organization and orientation differences of the different solution concentrations. For the aqueous solutions (Figure 1), the butanol ssp VSFG spectra reaches a maximum at 0.50 M, and the hexanol ssp VSFG spectra go through a maximum at 0.045 M.

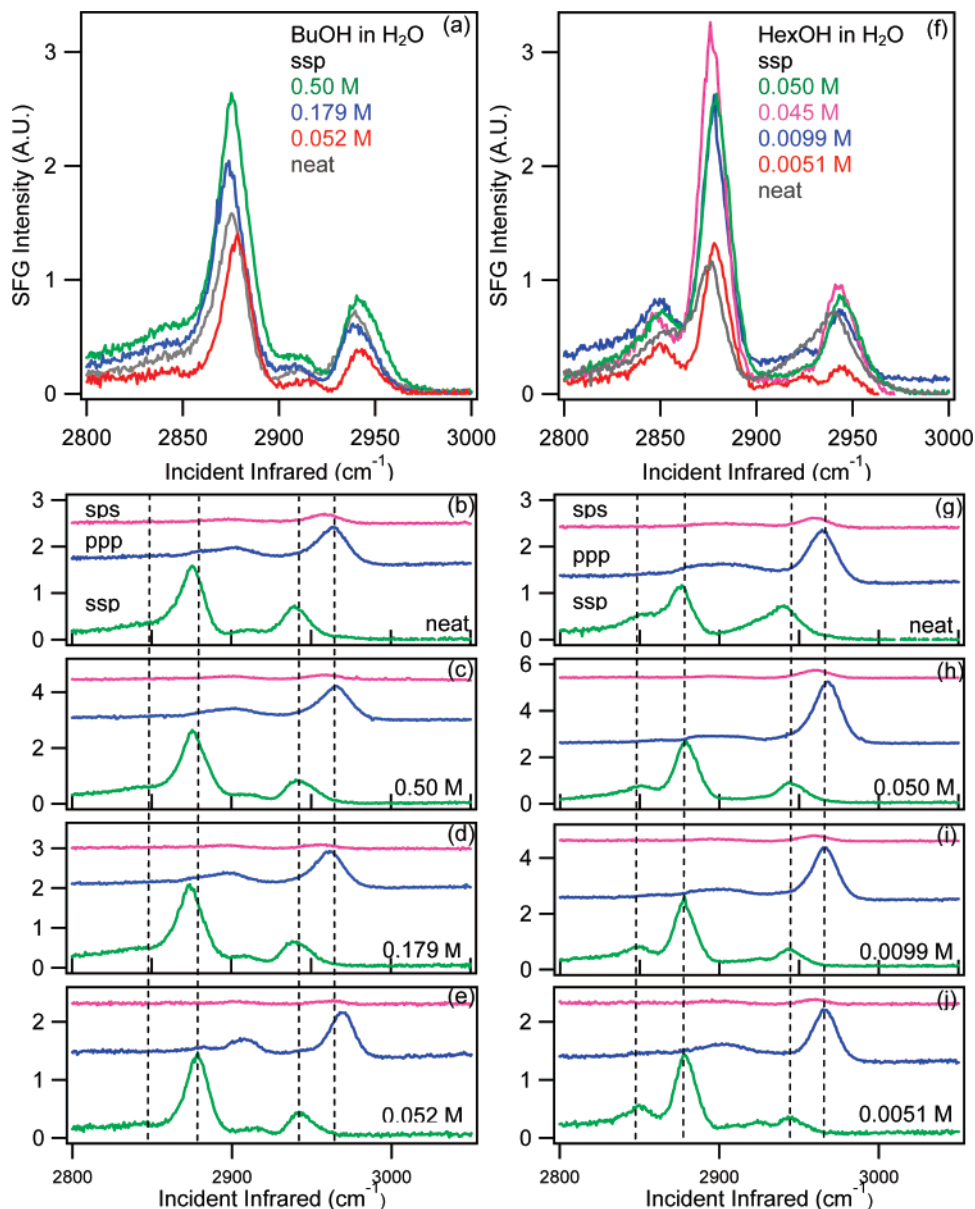


**Figure 1.** VSGF spectra of the CH stretching region of the (a–e) 1-butanol–water mixtures and (f–j) 1-hexanol–water mixtures. In parts b–e and g–j, the ssp spectra are shown in green, the ppp spectra are shown in blue, and the sps spectra are shown in pink. The dashed lines are guides for the eye showing peak position variation; from left to right for parts b–e and g–j are the CH<sub>2</sub>-ss, the CH<sub>3</sub>-ss, the CH<sub>3</sub>-FR, and the CH<sub>3</sub>-as, respectively.

The VSGF response, in particular the CH<sub>3</sub>-ss peak, for the neat solution surfaces is relatively small when compared to the higher concentration solutions. Previously, orientation differences have been used to explain the anticorrelation of the surface number density and the VSGF intensity of the CH<sub>3</sub>-ss.<sup>35</sup> Although this is still thought to be mostly true, the surface structure is more complex. Upon examination of the VSGF spectra in Figures 1–3, it is clear that centrosymmetry is playing a role in the reduced VSGF intensity of the CH<sub>3</sub>-ss from the neat butanol and neat hexanol surfaces. Orientation calculations (described further below and in the Supporting Information) do not account for the dramatic loss in VSGF signal intensity relative to the solution spectra in Figures 1–3. Thus, self-aggregation into surface structures that possess inversion symmetry is likely occurring. Inverse micelle-like structures are quite plausible at the neat alcohol surfaces. The alcohol moieties may form hydrogen-bonded aggregates that possess a certain degree of centrosymmetry. Upon addition of water, the alcohol

moieties hydrogen bond preferentially to the solvating water molecules, thereby breaking up the centrosymmetric surface aggregates.

Another plausible explanation for the relatively small intensity of the neat alcohols is centrosymmetry due to formation of layered hydrogen-bonded structures.<sup>42</sup> Simulations of neat octanol show the formation of hydrogen-bonded chains.<sup>43,42</sup> A molecular dynamics study of the *n*-octanol/vapor interface<sup>44</sup> show the alkyl chains aligned at the surface. Several layers beneath the interface these molecules are also well aligned due to hydrogen bonding between the hydroxyl groups. The weaker intensity of the neat alcohol ssp VSGF spectra is consistent with partial alignment of butanol and hexanol several layers into the interface, resulting in a cancellation of VSGF spectral intensity.

Comparing the neat alcohol ssp spectra (Figure 1a,f), the CH<sub>3</sub>-ss intensity of neat butanol is greater than that of neat hexanol. Perhaps hexanol, closer in length to octanol<sup>44</sup> than butanol, exhibits a stronger tendency to form inverse micelle-like surface

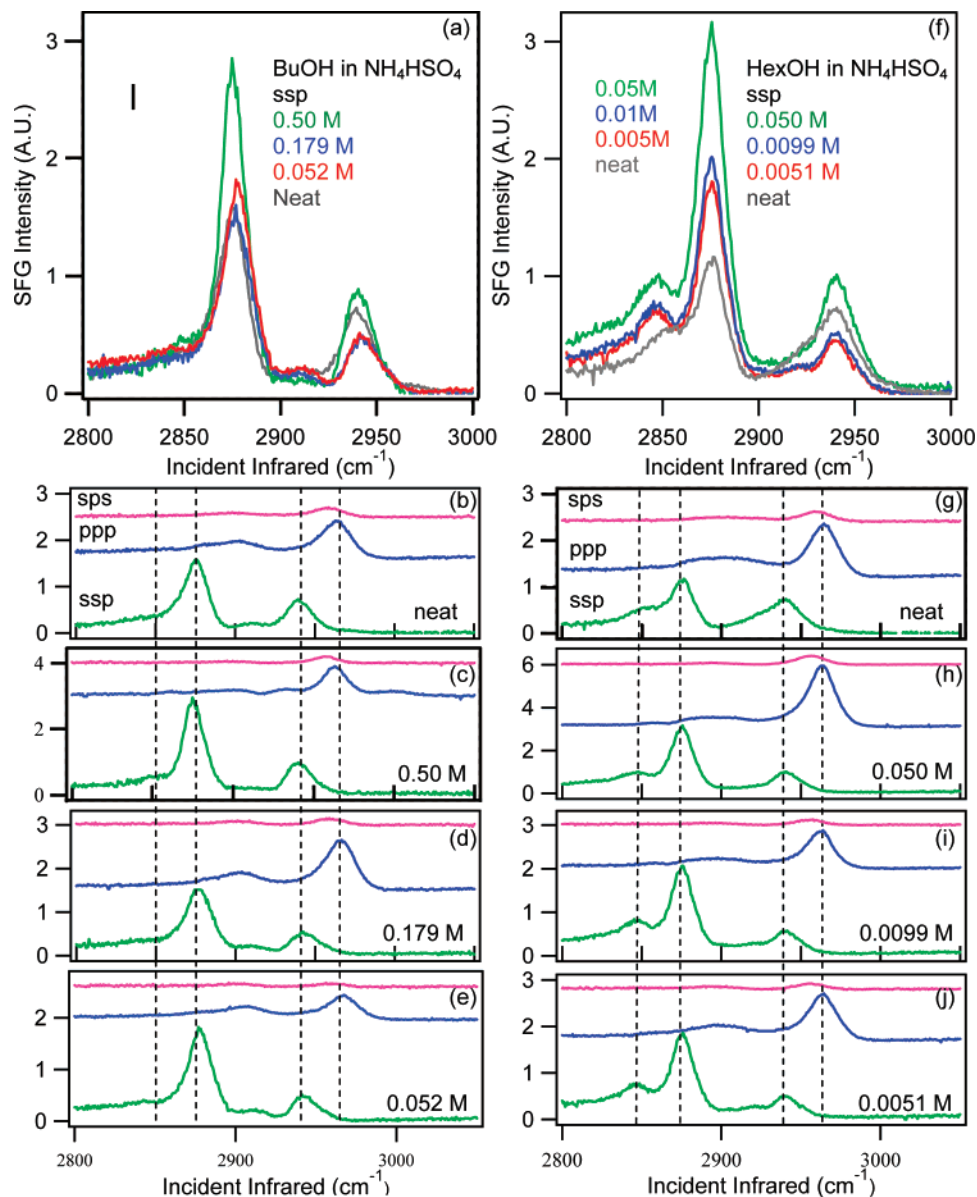


**Figure 2.** VSGF spectra of the CH stretching region of the (a–e) 1-butanol–0.78 M  $\text{NH}_4\text{HSO}_4$  mixtures and (f–j) 1-hexanol–0.78 M  $\text{NH}_4\text{HSO}_4$  mixtures. In parts b–e and g–j, the ssp spectra are shown in green, the ppp spectra are shown in blue, and the sps spectra are shown in pink. The dashed lines are guides for the eye showing peak position variation; from left to right for parts b–e and g–j are the  $\text{CH}_2$ -ss, the  $\text{CH}_3$ -ss, the  $\text{CH}_3$ -FR, and the  $\text{CH}_3$ -as, respectively.

structures or is somewhat better at forming multiple layered structures at the surface of its neat liquid. However, the additional presence of the  $\text{CH}_2$ -ss peak in the neat hexanol spectra (Figure 1f,g) makes the neat hexanol structure determination ambiguous.

A third contribution to the weaker intensity of the neat alcohols may be due to a broad distribution of the alkyl chains around the surface normal.<sup>31</sup> A broader distribution can be described by a Gaussian function rather than a  $\delta$  function. However, the peaks would then be expected to be broad relative to the solution surface spectra. This is not observed, consistent with Li et al.<sup>39</sup>

The influence of solvent on the alcohol surface organization of the butanol and hexanol solution spectra is shown in Figures 1–3. The most noticeable difference between the aqueous butanol and aqueous hexanol VSGF spectra is the significant presence of the  $\text{CH}_2$ -ss in the hexanol ssp spectra (Figures 1–3 (parts f–j)), and moreover, its near absence in the butanol spectra (Figures 1–3 (parts a–e)), with the exception of the anomalous 0.052 M butanol in SA spectrum (Figure 3a,e).

Presence of methylene VSGF intensity is an important indicator of gauche conformations, and therefore, ordering, or rigidity, of the alkyl chains.<sup>30</sup> In an all-trans alkyl chain, local inversion centers disallow the SFG response, as is observed in the butanol spectra shown in Figures 1–3 (except the 0.052 M BuOH in SA). However, gauche defects destroy the local centrosymmetric methylene structures and thereby the  $\text{CH}_2$  modes in an alkyl chain become SFG-active. For hexanol, the  $\text{CH}_2$ -ss is observed in all spectra (Figures 1–3), indicating that hexanol molecules possess a significant number of gauche defects in their alkyl chains. Hexanol is disordered at the neat, aqueous, aqueous ammonium bisulfate and 59.5 wt % SA surfaces.

Using the fitted intensities of the  $\text{CH}_3$  and  $\text{CH}_2$  symmetric stretches in the ssp spectra, the  $\text{CH}_3$ -ss/ $\text{CH}_2$ -ss ratios ( $I_{\text{CH}_3}/I_{\text{CH}_2}$ ) can be calculated for each butanol and hexanol solution. This ratio (or its inverse) is used as a measure of gauche defects.<sup>45</sup> Large  $\text{CH}_3$ -ss/ $\text{CH}_2$ -ss ratios indicate order, whereas small ratios indicate disorder in the alkyl chains. Although this indicator can be convoluted by a methyl orientation effect, it provides

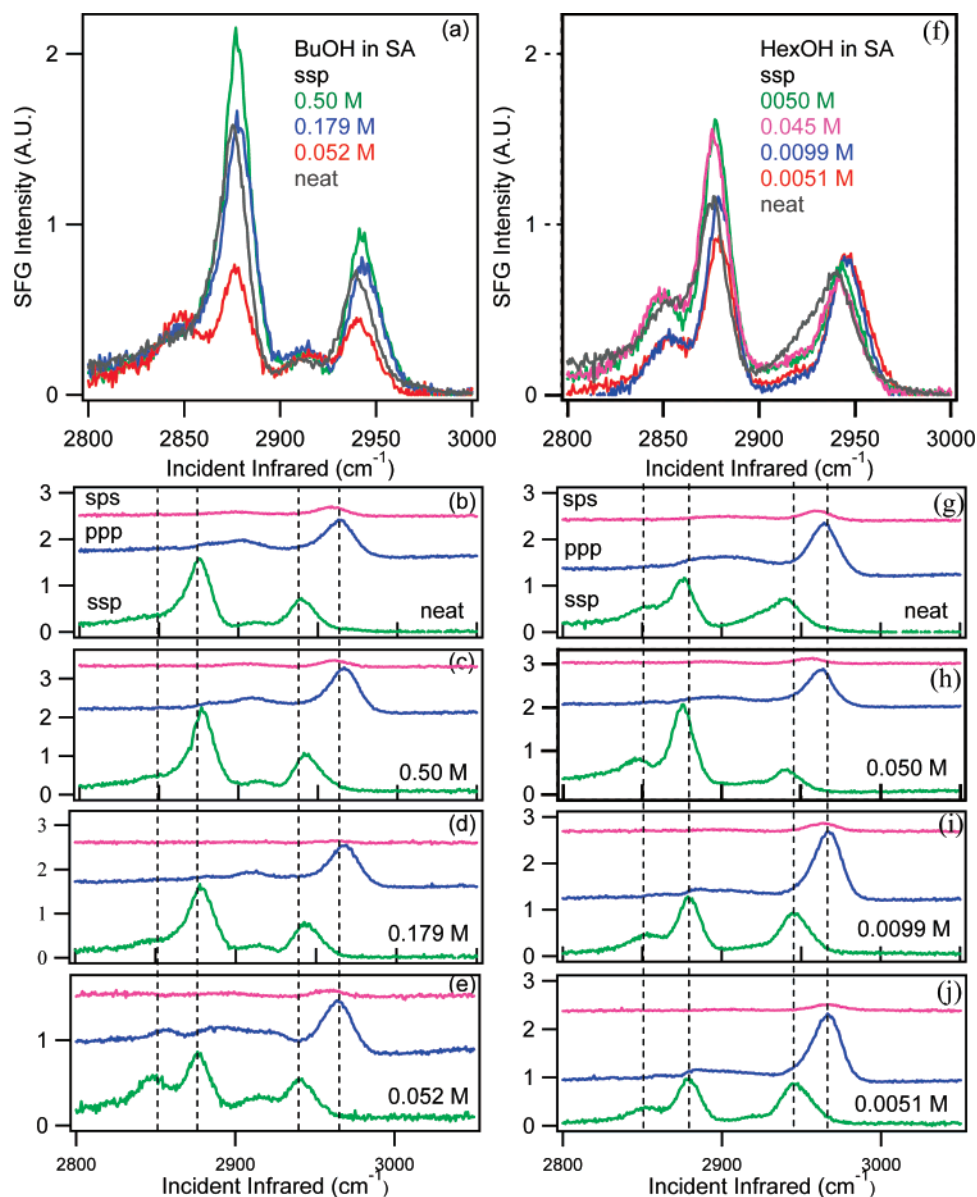


**Figure 3.** VSGF spectra of the CH stretching region of the (a–e) 1-butanol–59.5 wt % SA mixtures and (f–j) 1-hexanol–59.5 wt % SA mixtures. In parts b–e and g–j, the ssp spectra are shown in green, the ppp spectra are shown in blue, and the sps spectra are shown in pink. The dashed lines are guides for the eye showing peak position variation; from left to right for parts b–e and g–j are the CH<sub>2</sub>-ss, the CH<sub>3</sub>-ss, the CH<sub>3</sub>-FR, and the CH<sub>3</sub>-as, respectively.

**TABLE 1: Calculated  $I_{\text{CH}_3}/I_{\text{CH}_2}$  Ratio for the 1-Hexanol Solutions and the 0.052 M 1-butanol in SA Solution**

	neat HexOH	0.050 M HexOH	0.045 M HexOH	0.0099 M HexOH	0.0051 M HexOH	0.052 M BuOH
			In Water			
$I_{\text{CH}_3}/I_{\text{CH}_2}$	7.3	14.0	18.0	9.2	9.0	
			In 0.78 M NH <sub>4</sub> HSO <sub>4</sub>			
$I_{\text{CH}_3}/I_{\text{CH}_2}$		7.3		5.7	5.3	
			In 59.5 wt % SA			
$I_{\text{CH}_3}/I_{\text{CH}_2}$		6.5	3.0	12.1	7.2	2.5

additional evidence for order vs disorder. In Table 1, hexanol  $I_{\text{CH}_3}/I_{\text{CH}_2}$  ratios and the 0.052 M butanol in SA ratio are shown. The hexanol solutions have ratios less than 20. We were unable to confirm the presence of any VSFG CH<sub>2</sub>-ss intensity for the butanol solution spectra, including neat butanol, and therefore, we do not report ratios for these solutions; they are clearly large for the butanol spectra, indicating that surface butanol may exist in all-trans conformations (the alkyl chains are well ordered).

Hexanol has two additional methylene groups relative to butanol, and statistically, it has a greater possibility of producing

gauche conformations. Therefore, one would expect additional methylene intensity for hexanol relative to butanol. This is consistent with previous work by Stanners et al.<sup>31</sup> and Nicholov et al.<sup>46</sup>

Another possible explanation to our observation that butanol is significantly more ordered than hexanol at the surface of aqueous solutions stems from potential solvent interactions with butanol vs hexanol. Butanol has a shorter chain, and energetically it should be less favorable for the butanol chain to contain gauche configurations, which would tilt the terminal methyl

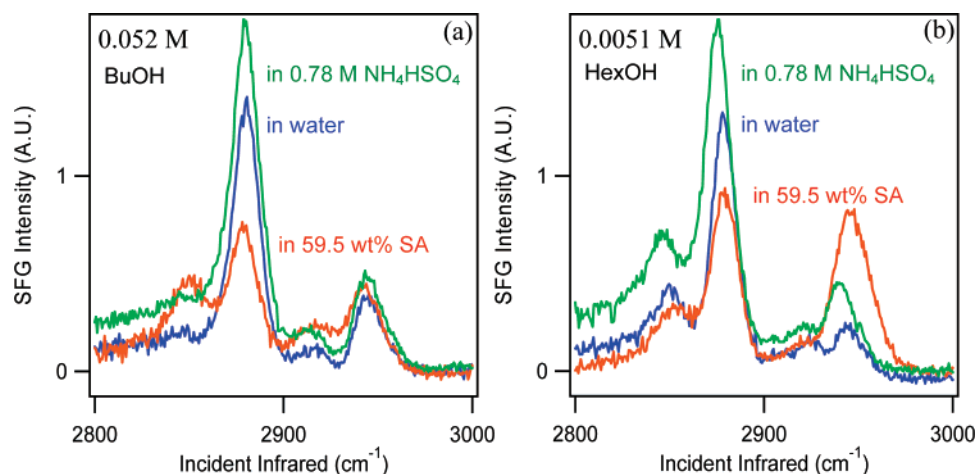


**Figure 4.** VSFG ssp polarization spectra of (a) 0.052 M 1-butanol solution and (b) 0.0051 M 1-hexanol solution. The water solutions are shown in blue, the 0.78 M  $\text{NH}_4\text{HSO}_4$  solutions are shown in green, and the 59.5 wt % SA solutions are shown in orange.

group back toward the surface. In hexanol, the conformation with  $\text{C}_3$  gauche to the oxygen is the lowest energy conformation.<sup>47</sup> Raman spectroscopy studies showed that the energy differences between all-trans and trans-gauche conformations of 1-pentane are much smaller than the energy differences for 1-butane.<sup>48</sup> Following these results, the energy difference between all-trans and trans-gauche conformations for hexanol chains should then be smaller than that for butanol chains.

The conformational energies of butanol in water have been investigated using ab initio molecular orbital calculations and Raman spectroscopy.<sup>49</sup> Raman spectra revealed that the gauche conformers of butanol dominate in aqueous solutions in order to minimize the butanol surface area that is in contact with water molecules. Using this argument, it is plausible to postulate that at the aqueous surface, butanol prefers an all-trans conformation to minimize the interaction between the alkyl chain and surface water.

The lack of  $\text{CH}_2$ -ss intensity in the butanol spectra as compared with the hexanol spectra may also be due to a larger orientation distribution of the butanol molecules around the surface normal. This was also discussed above as a possible explanation for the neat alcohol spectral differences. In addition to the Stanners et al.<sup>31</sup> study that suggests this, an AFM study of butanol and hexanol adsorbed onto a mica surface<sup>50</sup> showed that the surface butanol chains were more randomly oriented than the surface hexanol chains. However, spectral broadening of the butanol peaks is not observed relative to the hexanol peaks, which leads one to conclude that the orientation distribution is similar for both alcohols. This is consistent with a neutron reflection study by Li et al. that found that butanol and hexanol have similar distributions.<sup>39</sup>

Comparison of the butanol spectra in water, aqueous ammonium bisulfate, and most of the SA solutions, reveal that the  $\text{CH}_2$ -ss remains absent from the spectra. The butanol molecules stay in their all-trans conformation even at low surface excess. Orientation calculations using the ssp and ppp spectral intensities also reveal that the chain tilt angles are between 4 and 13° from the surface normal for butanol in aqueous, in aqueous ammonium bisulfate, and in SA solutions (except the 0.052 M BuOH in SA). (Orientation calculation data is available in the Supporting Information.) Butanol molecules do not change their orientation or surface organization to any significant extent with solvent variation. There may be self-aggregation at the surface of these butanol solutions that stabilizes the rigid butanol structures. This is in contrast to the individual alcohol molecules spreading out in an isolated fashion evenly over the entire

surface. Consistent with this hypothesis, propanol studies show that even at very low concentrations, the alcohol molecules self-aggregate into clusters.<sup>51</sup> Additionally, an investigation of a saturated butanol-water solution showed that both self-aggregated clusters and butanol clusters with hydrogen-bonded water molecules exist.<sup>52</sup>

Molecular modeling of the water-butanol surface predict that the alkyl chains of butanol are aligned upright, and that the presence of water enhances ordering compared to that of neat butanol.<sup>15</sup> We observe a significant difference in the neat (21.5°) vs solution butanol chain orientation (4–13°), consistent with Chen et al.<sup>15</sup> Electric surface potential measurements<sup>53</sup> suggest that *n*-butanol molecules adsorbed to the surface of water are nearly perpendicular in order to prevent the hydrophobic chain from coming into contact with the water. These experimental and theoretical results as discussed above are consistent with the findings and interpretation presented here.

The ratios in Table 1 reveal that hexanol is disordered at its solution surfaces. In the low concentration regime in water (0.0051 and 0.0099 M), the  $I_{\text{CH}_3}/I_{\text{CH}_2}$  values are in the single digits, indicative of disorder. Ratios in the full surface coverage concentration regime (0.045 and 0.052 M) become larger by about a factor of 2, indicating that the increased surface coverage helps to minimize the existing gauche conformations, stabilizing the hexanol alkyl chain to some extent. This is not observed in the aqueous ammonium bisulfate or SA solutions for hexanol, revealing that the solvent is playing a significant role in the surface ordering, or lack thereof, for hexanol. Chain tilt angle calculations will be inaccurate for these solutions since the methyl tilt angle is not representative of the chain tilt due to the gauche conformations in the hexanol chains.

As discussed above, ordering of the butanol molecules at the surface of the various solutions is constant and well ordered, quite different relative to hexanol surfaces. However, the 0.052 M butanol in 59.5 wt % SA has a  $I_{\text{CH}_3}/I_{\text{CH}_2}$  of 2.5, close to the  $I_{\text{CH}_3}/I_{\text{CH}_2}$  from hexanol at the surface of the 0.045 M hexanol in 59.5 wt % SA, revealing that these surfaces are the most disordered of the alcohol surfaces studied here.

To understand how these alcohols could organize at the surface of sulfate-containing atmospheric aerosols, the differences in surface structure with water vs ammonium bisulfate vs SA solution as solvent is examined. The presence of salts in aqueous solutions can reduce the solubility of organic compounds such as alcohols. This is known as the salting out effect.<sup>54,55</sup> Previous surface tension experiments of 1-propanol in aqueous NaCl solutions show a greater decrease in surface

tension at low propanol and high salt concentrations, indicating that salting out occurs.<sup>56</sup> Here, the VSFG spectra of the two lowest surface excess concentrations shown in Figure 4a,b show evidence for salting out of butanol and hexanol. The CH<sub>3</sub> symmetric stretches are more intense in the ammonium bisulfate solutions than in the water solutions.

The intensity of the 59.5 wt % SA solutions is lower than that of the water solutions as is shown in Figure 4a,b (other concentration spectra are shown in Supporting Information). Unlike for the water solutions, no solubility limit for butanol and hexanol in SA was observed, both in this work and in previous studies.<sup>13</sup> In 60 wt % SA solution, using the pK<sub>a</sub> of ethanol (−1.94)<sup>57</sup> and a value of H<sub>ROH</sub> of −1.59<sup>57</sup> and assuming an equilibrium constant of 0.31<sup>58</sup> we calculate a distribution of 57% BuOH (HexOH), 25% BuOH<sub>2</sub><sup>+</sup> (HexOH<sub>2</sub><sup>+</sup>), and 18% BuOSO<sub>3</sub>H/BuOSO<sub>3</sub><sup>−</sup> (HexOSO<sub>3</sub>H/HexOSO<sub>3</sub><sup>−</sup>). However, this speciation does not appear to affect the surface CH<sub>3</sub>-ss vibrational frequency. The calculated surface excess for butanol in SA is lower than that for butanol in water,<sup>37</sup> and it is likely that this is the case for hexanol as well. The surface structure of the 0.052 M butanol in SA solution is different from the other butanol solutions. This is apparent from the presence of the CH<sub>2</sub>-ss in the ssp spectrum. This may indicate that the butanol is not aggregating to the same extent as at the other solution surfaces.

## Conclusions

The organization of 1-butanol and 1-hexanol molecules at the air–liquid interface of water, aqueous NH<sub>4</sub>HSO<sub>4</sub>, and 59.5 wt % sulfuric acid solutions was investigated using vibrational broad bandwidth sum frequency generation spectroscopy. The VSFG spectra strongly suggest that aggregation into somewhat centrosymmetric structures of the neat butanol and neat hexanol molecules is occurring at the neat surfaces. Butanol is relatively rigid, with all-trans chains for all solution surfaces investigated, with the exception of low concentration butanol in sulfuric acid. Hexanol, on the other hand, appears to contain gauche defects in its chain for all solution surfaces investigated. Statistically, hexanol is expected to contain more gauche defects. Energy arguments at the aqueous surface are consistent with this as well. Methylene peak intensities from hexanol are still relatively small compared to the response from the hexanol methyl groups, indicating that the number of gauche defects is likely small for most hexanol solutions. Butanol, and for that matter, hexanol, may self-aggregate at the solution surfaces to help maintain their somewhat rigid surface structures. However, energetically, butanol is more likely to be in all-trans conformations relative to hexanol at the solution surfaces due to potential and unfavorable solvent interactions.

**Acknowledgment.** The authors greatly acknowledge the National Science Foundation for financial support (NSF–CAREER CHE-0134131). The authors thank Dr. G. Ma for assistance.

**Supporting Information Available:** Text discussing the ssp, ppp, and sps VSFG spectra fit with the component peaks, tables of both the peak assignments and fitted peak positions, and figures of the spectra normalized to the CH<sub>3</sub>-ss, figures comparing the effect of the different solvents, the input parameters used for the orientation calculations, and an example orientation angle plot. This material is available free of charge via the Internet at <http://pubs.acs.org>.

## References and Notes

- (1) Kerminen, V.-M.; Anttila, T.; Lehtinen, K. E. J.; Kulmala, M. *Aerosol Sci. Technol.* **2004**, *38*, 1001–1008.
- (2) Facchini, M. C.; Decesari, S.; Mircea, M.; Fuzzi, S.; Loglio, G. *Atmos. Environ.* **2000**, *34*, 4853–4857.
- (3) Facchini, M. C.; Mircea, M.; Fuzzi, S.; Charlson, R. J. *Nature (London)* **1999**, *401*, 257–259.
- (4) Murphy, D. M.; Thomson, D. S.; Mahoney, M. J. *Science* **1998**, *282*, 1664–1669.
- (5) Singh, H.; Chen, Y.; Staudt, A.; Jacob, D.; Blake, D.; Heikes, B.; Snow, J. *Nature (London)* **2001**, *410*, 1078–1081.
- (6) Donaldson, D. J.; Vaida, V. *Chem. Rev.* **2006**, *106*, 1445–1461.
- (7) Noziere, B.; Esteve, W. *Geophys. Res. Lett.* **2005**, *32*, L03812, doi: 10.1029/2004GL021942.
- (8) Alexander, A. *Rep. Prog. Phys.* **1942**, *9*, 158–176.
- (9) Alexander, A. *Proc. R. Soc. London, Ser. A* **1942**, *179*, 486–499.
- (10) Glass, S. V.; Park, S.-C.; Nathanson, G. M. *J. Phys. Chem. A* **2006**, *110*, 7593–7601.
- (11) Sung, J.; Park, K.; Kim, D. *J. Phys. Chem. B* **2005**, *109*, 18507–18514.
- (12) Finlayson-Pitts, B. J.; Pitts, J.; James, N. *Chemistry of the Upper and Lower Atmosphere*; Academic Press: San Diego, CA 2000.
- (13) Torn, R. D.; Nathanson, G. M. *J. Phys. Chem. B* **2002**, *106*, 8064–8069.
- (14) Gao, J.; Jorgensen, W. L. *J. Phys. Chem.* **1988**, *92*, 5813–5822.
- (15) Chen, B.; Siepmann, J. I.; Klein, M. L. *J. Am. Chem. Soc.* **2002**, *124*, 12232–12237.
- (16) Lawrence, J. R.; Glass, S. V.; Nathanson, G. M. *J. Phys. Chem. A* **2005**, *109*, 7449–7457.
- (17) Lawrence, J. R.; Glass, S. V.; Park, S.-C.; Nathanson, G. M. *J. Phys. Chem. A* **2005**, *109*, 7458–7465.
- (18) Thornton, J. A.; Abbott, J. P. D. *J. Phys. Chem. A* **2005**, *109*, 10004–10012.
- (19) Johnson, C. M.; Tyrode, E.; Baldelli, S.; Rutland, M. W.; Leygraf, C. *J. Phys. Chem. B* **2005**, *109*, 321–328.
- (20) Shultz, M. J.; Baldelli, S.; Schnitzer, C.; Simonelli, D. *J. Phys. Chem. B* **2002**, *106*, 5313–5324.
- (21) Tarbuck, T. L.; Richmond, G. L. *J. Am. Chem. Soc.* **2006**, *128*, 3256–3267.
- (22) Van Loon, L. L.; Allen, H. C. *J. Phys. Chem. B* **2004**, *108*, 17666–17674.
- (23) Voss, L. F.; Hadad, C. M.; Allen, H. C. *J. Phys. Chem. B* **2006**, *110*, 19487–19490.
- (24) Lambert, A. G.; Davies, P. B.; Neivandt, D. J. *Appl. Spectrosc. Rev.* **2005**, *40*, 103–145.
- (25) Moad, A. J.; Simpson, G. J. *J. Phys. Chem. B* **2004**, *108*, 3548–3562.
- (26) Shen, Y.-R. *Surf. Sci.* **1994**, *299–300*, 551–562.
- (27) Zhuang, X.; Miranda, P. B.; Kim, D.; Shen, Y.-R. *Phys. Rev. B* **1999**, *59*, 12632–12640.
- (28) Lu, R.; Gan, W.; Wu, B.-h.; Zhang, Z.; Guo, Y.; Wang, H.-f. *J. Phys. Chem. B* **2005**, *109*, 14118–14129.
- (29) Hirose, C.; Akamatsu, N.; Domen, K. *Appl. Spectrosc.* **1992**, *46*, 1051–1072.
- (30) Ma, G.; Allen, H. C. *Langmuir* **2006**, *22*, 5341–5349.
- (31) Stanners, C. D.; Du, Q.; Chin, R. P.; Cremer, P.; Somorjai, G. A.; Shen, Y.-R. *Chem. Phys. Lett.* **1995**, *232*, 407–413.
- (32) Wang, H.-f.; Gan, W.; Lu, R.; Rao, Y.; Wu, B.-H. *Int. Rev. Phys. Chem.* **2005**, *24*, 191–256.
- (33) Ye, S.; Noda, H.; Nishida, T.; Morita, S.; Osawa, M. *Langmuir* **2004**, *20*, 357–365.
- (34) Hommel, E. L.; Ma, G.; Allen, H. C. *Anal. Sci.* **2001**, *17*, 137–139.
- (35) Ma, G.; Allen, H. C. *J. Phys. Chem. B* **2003**, *107*, 6343–6349.
- (36) Ma, G.; Allen, H. C. *Photochem. Photobiol.* **2006**, *82*, 1517–1529.
- (37) Nathanson, G. M. Personal communication.
- (38) Chen, H.; Gan, W.; Lu, R.; Guo, Y.; Wang, H.-f. *J. Phys. Chem. B* **2005**, *109*, 8064–8075.
- (39) Li, Z. X.; Lu, J. R.; Thomas, R. K.; Rennie, A. R.; Penfold, J. J. *Chem. Soc., Faraday Trans.* **1996**, *92*, 565–572.
- (40) Tomasson, M. S.; Couzis, A.; Maldarelli, C. M.; BAnavar, J. R.; Koplik, J. *J. Chem. Phys.* **2001**, *115*, 8364–8642.
- (41) Physical Constants of Organic Compounds. In *CRC Handbook of Chemistry and Physics, Internet Version 2007*, 87th ed.; Lide, D. R., Ed.; Taylor and Francis: Boca Raton, FL 2007.
- (42) MacCallum, J. L.; Tieleman, D. P. *J. Am. Chem. Soc.* **2002**, *124*, 15085–15093.
- (43) Chen, B.; Siepmann, J. I. *J. Phys. Chem. B* **2006**, *110*, 3555–3563.
- (44) Napoleon, R. L.; Moore, P. B. *J. Phys. Chem. B* **2006**, *110*, 3666–3673.



- (45) Conboy, J. C.; Messmer, M. C.; Richmond, G. L. *J. Phys. Chem. B* **1997**, *101*, 6724–6733.
- (46) Nickolov, Z. S.; Wang, X.; Miller, J. D. *Spectrochim. Acta A* **2004**, *60*, 2711–2717.
- (47) Houk, K. N.; Eksterowicz, J. E.; Wu, Y.-D.; Fuglesang, C. D.; Mitchell, D. B. *J. Am. Chem. Soc.* **1993**, *115*, 4170–4177.
- (48) Tsuzuki, S.; Uchimaru, T.; Tanabe, K. *Chem. Phys. Lett.* **1995**, *246*, 9–12.
- (49) Ohno, K.; Yoshida, H.; Watanabe, H.; Fujita, T.; Matsuura, H. *J. Phys. Chem.* **1994**, *98*, 6924–6930.
- (50) Wang, L.; Song, Y.; Zhang, B.; Wang, E. *Thin Solid Films* **2004**, *458*, 197–202.
- (51) Wakisaka, A.; Komaisu, S.; Usui, Y. *J. Mol. Liq.* **2001**, *90*, 175–184.
- (52) Wakisaka, A.; Mochizuki, S.; Kobara, H. *J. Sol. Chem.* **2004**, *33*, 721–732.
- (53) Dynarowicz, P. *Colloids Surf.* **1989**, *42*, 39–48.
- (54) Bowren, D. T.; Finney, J. L. *Phys. Rev. Lett.* **2002**, *89*, 215508.
- (55) Daiguji, H. *J. Chem. Phys.* **2001**, *115*, 1538–1549.
- (56) Demou, E.; Donaldson, D. J. *J. Phys. Chem. A* **2002**, *106*, 982–987.
- (57) Lee, D. G.; Cameron, R. *J. Am. Chem. Soc.* **1971**, *93*, 4724–4728.
- (58) Clark, D. J.; Williams, G. *J. Chem. Soc.* **1957**, 4218–4221.